COBEM 2023 27TH INTERNATIONAL CONGRESS OF MECHANICAL ENGENEERING

ABCM Brazilian Society of Mechanical Sciences and Engineering
27th ABCM International Congress of Mechanical Engineering
December 04-08, 2023, Florianópolis-SC, Brazil

COBEM-2023-2145
EXPERIMENTAL ANALYSIS OF THE DESALINATION PROCESS BY VACUUM ENHANCED AIR GAP MEMBRANE DISTILLATION IN A PILOT SYSTEM

Ingrid Vasconcelos Curcino
Thomás R. P. Costa
Guilherme de Oliveira Rosa
Abdul O. C. Gómez
Carolina Palma Naveira-Cotta
Laboratory of Nano & Microfluidics and Microsystems - LabMEMS, Mechanical Eng. Dept.,POLI & COPPE/UFRJ, Federal University of Rio de Janeiro, RJ, Brazil
carolina@mecanica.coppe.ufrj.br

Renato M. Cotta
Laboratory of Nano & Microfluidics and Microsystems - LabMEMS, Mechanical Eng. Dept.,POLI & COPPE/UFRJ, Federal University of Rio de Janeiro, RJ, Brazil
Laboratory of Technologies for Sustainable Energies, LATES, Materials Technology Group, Navy Research Institute, IPqM, General Directorate of Nuclear and Technological Development, DGDNTM, Brazilian Navy, Rio de Janeiro, RJ, Brazil
cotta@mecanica.coppe.ufrj.br

Abstract. *The present study aimed to experimentally investigate the effects of the operating parameters (factors): feed inlet temperature (56.6 °C - 73.4 °C), circulation flow rate (331.8 L/h - 668.2 L/h), and air gap manometric average pressure (-231.8 mbar -568.2 mbar) on the performance parameters: distillate flux, specific thermal energy consumption (SECth) and gain output ratio (GOR) of the membrane distillation process of a 35 g/L NaCl solution from a V-AGMD (Vacuum-enhanced Air Gap Membrane Distillation) spiral module, according to a central composite experimental design. The statistical analysis, for the studied operating range, indicated that the feed inlet temperature and the circulation flow rate are the most statistically significant parameters on the considered performance parameters. For the distillate flux, these two factors showed a positive and synergistic effect on the increase in distillate production. For the SECth, the lowest values of this parameter were obtained when increasing the feed inlet temperature and decreasing the circulation flow rate. While for the GOR, a reduction was observed when decreasing the feed inlet temperature and increasing the circulation flow rate. To preliminarily evaluate the ability to process solutions with higher concentrations, experiments were conducted with 70 g/L NaCl solution for four fixed operational conditions. These additional experiments indicated a reduction of 28.57% of the distillate flux (compared to the experiments with 38±5 g/L NaCl) and a rejection of 91% of the salt, indicating the ability to process high salt concentration waste solutions such as those from reverse osmosis.*

Keywords: *Desalination, VAGMD, Distillate Flux, Specific Thermal Energy Consumption, Gain output ratio.*

1. INTRODUCTION

The increasing scarcity of quality water, because of population growth, overexploitation of water resources, and climate change, has motivated the use of desalination technologies to remove salts from water sources (e.g., seawater and brackish water) to facilitate access to fresh water, either for human consumption or industrial activities (World Health Organization, 2017). However, desalination is an energy demanding process, which can be a problem for its implementation in remote communities .(Yadav et al., 2021). In this context, the membrane distillation process has been studied as a promising alternative desalination process to be combined with low energy heat recovery systems.

One of the main advantages of membrane distillation as a desalination process is its high selectivity and ability to operate at lower temperatures than other traditional thermal desalination processes, e.g., distillation (Deshmukh et al., 2018). Thus, the coupling of the membrane distillation process with low energy waste heat sources has been studied as an alternative to enable desalination with membrane distillation at lower cost by using low energy waste heat sources such as solar energy, geothermal energy, waste heat from ships, industries, and power stations (Koschikowski et al., 2003; Sarbatly and Chiam, 2013; Bahar, Ng, 2020).

Membrane distillation is a hybrid desalination process because it is a thermal process intermediated by a hydrophobic, porous membrane. In the V-AGMD (Vacuum-enhanced Air Gap Membrane Distillation) configuration, a space of

stagnant air at a pressure lower than atmospheric pressure exists between one of the membrane surfaces and the condenser plate (which is cooled by a cooling fluid). The partial vacuum promotion in the air gap decreases the mass transfer resistance by removing non-condensable gases while maintaining the reduction of heat losses by conduction through the membrane. In this configuration, the volatile component evaporates at the interface between the heated feed stream and the membrane surface. Then, the vapor is transported through the membrane pores and the air gap, in the distillate channel, toward the cooled surface of the condenser plate. The vapor is condensed and collected at the base of the module (Khayet and Matsuura, 2011; Khayet and Cojocaru, 2012; Alsaadi et al., 2015; Abu-Zeid et al., 2016).

In addition, since the cooling stream is not in direct contact with the membrane surface, it allows the feed solution to be used as the cooling stream. As a result, there is internal recovery of the latent heat of evaporation during condensation of the vapor in the condenser plate, as the feed solution flows into the cooling channel. Recently, Andrés-Mañas et al. (2020) and Andrés-Mañas et al. (2022) demonstrated, at pilot scale and controlled heating conditions, that the use of a spiral module with the V-AGMD configuration allowed for both increased distillate flux and reduced specific thermal energy and electrical energy consumption.

In the Brazilian context, the desalination plants installed by the "Programa Água Doce" (Brasil, 2012) in the northeast region use the reverse osmosis (RO) process which has, as its driving force, a high-pressure gradient that causes significant consumption of electrical energy. Reverse osmosis (RO) modules use a dense, selective, semi-permeable membrane that restricts the passage of one or more chemical species from the feed reservoir to the permeate fluid (desalinated water), producing a high concentration reject. Hence, in reverse osmosis desalination, for feed streams with concentrations of around or greater than 35g/l of NaCl, the membranes used can treat about 30% to 40% of the volume of water extracted (permeate) and the rest (concentrate) of 60% to 70% is rejected without any treatment (Sanmartino et al., 2017; Schwantes et al., 2018; Jones et al., 2019).

In this regard, the desalination process by membrane distillation (MD) offers an opportunity to integrate with already installed technologies, for the treatment and reprocessing of highly concentrated waste (with concentrations of up to 150 g/L of NaCl) improving the use of often scarce water resources and increasing the rate of water recovery (Ong et al., 2012; Chafidz et al., 2014; Wiesenfarth et al., 2016; Bindels et al., 2020).

In view of the advantages offered by the V-AGMD configuration combined with the compactness of the spiral module, the present study aimed to experimentally investigate the effect of operating parameters (factors): feed inlet temperature (56.6 °C - 73.4 °C), circulation flow rate (331.8 L/h - 668.2 L/h), and air gap manometric average pressure (between -231.8 mbar and -568.2 mbar) on the production performance (distillate flux) and thermal efficiency parameters (specific thermal energy consumption and gain output ratio) of the membrane distillation process of a 35 g/L NaCl solution (value close to that of seawater) using a V-AGMD spiral module in a pilot unit installed at LabMEMS/COPPE/UFRJ, according to a central composite experimental design. Additionally, four complementary experiments were performed with a high concentration salt solution (approximately 70 g/L of NaCl) in order to perform a preliminary evaluation of the membrane distillation modules ability to process fluids rejected by reverse osmosis (RO) desalination processes, offering an alternative to increase the water recovery rate and build the management of desalination process rejects.

2. EXPERIMENTAL METHODOLOGY

The methodology described below was used to analyze the membrane distillation desalination process in the V-AGMD configuration using NaCl aqueous solution with a nominal concentration of 35 g/L as the feed stream solution.

The membrane distillation process was evaluated in a relevant environment using a pilot desalination unit PURA-1 system (production capability up to 1 m^3/day) from the Dutch company Aquastill (Aquastill PURA-1 System - Aquastill, n.d.). The system operated with the PLICA13 module in AGMD/V-AGMD configurations. The desalination process was carried out from the heat provided by a system of flat solar collectors combined with an electrical resistance with power equal to 5kW. A schematic illustration of the MD process in the Pura1 unit is presented in Figure 1, which has the necessary instrumentation (temperature, pressure, flow rate, and electrical conductivity transmitters) for the experimental characterization.

The V-AGMD spiral module contains only one inlet and one outlet for the corresponding feed and cooling streams, and one outlet for the distillate. However, it is internally subdivided into six evaporation channels, six cooling channels, and 12 distillate channels. The module has a total membrane area of 12.96 m^2, and the length of each channel is equal to 2.7 m. The width of the evaporation and cooling channels is provided by PP (Polypropylene) spacers, with a thickness of 2 mm, porosity equal to 86.02%, and attack angle equal to 68°. The distillate channels, in which there is an air gap, are separated by spacers with a thickness of 0.8 mm, an angle between the filaments of 90°, and a porosity equal to 90.6%. The surface where the condensation of the distillate vapor occurs consists of an aluminum foil coated on both sides with PET (Polyethylene terephthalate) and a thickness of 62 μm that separates the distillate channel from the cold stream channel. The membrane used consists of PE (polyethylene) with a thickness equal to 100 μm, porosity equal to 85%, and average pore diameter equal to 0.32 μm.

The operation of the pilot desalination system used in this study is illustrated in Figure 1. Initially, the feed solution enters the cooling channels of the V-AGMD PLICA13 module at the cooling temperature maintained around 30°C. Then,

the feed solution exits the cooling channels preheated by internal heat recovery and flows into the external heat exchanger (HX in Figure 1). The heat supplied by the heat absorption circuit (highlighted by red dotted rectangle in Figure 1) came from the coupling of six LIRA 200 flat plate solar thermal collectors from company SOLAREM, with a total effective area of 12 m², combined with a Kisoltec vertical thermal storage tank (300 liters) with an electrical resistance with power equal to 5kW. In this study the solar thermal collectors were used only to supplement the thermal energy transferred to the desalination system (highlighted by gray dotted rectangle in Figure 1) during the experiments. The transient effect of solar irradiation was not considered in this study of controlled conditions for the membrane distillation process.

The external heat exchanger (HX in Figure 1) transfers the heat absorbed from the heat absorption circuit to the salt solution to achieve the feed inlet temperature selected for each experimental condition and which was varied according to the experimental design matrix. Two 3-way valves (VH and VC in Figure 1) were used to control the feed inlet and cooling inlet temperatures. Actuating these valves provided control over the energy transferred in the heat exchangers. The desalination unit has an automated fluid supply and discharge system in the internal feed tank. It keeps the concentration of the feed solution at desired levels by monitoring the electrolytic conductivity of the solution. The monitoring, control, and recording of process variables such as temperature, circulation flow rate, pressure, volume of water produced, and electrolytic conductivity are performed by the data acquisition system for post-processing the information collected in the experiment.

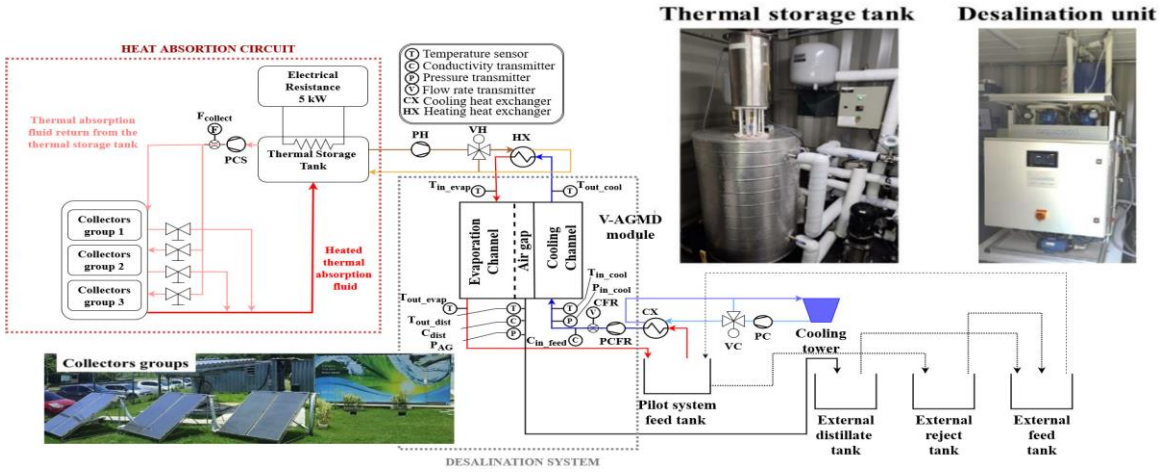

Figure 1. Schematic representation of the pilot solar desalination system operation circuit.

For the experimental evaluation of the membrane distillation process with the spiral module in the V-AGMD configuration, the experiments were performed according to a central composite design, with a matrix of experiments presented in Table 1.

Table 1. Central composite design matrix.

Run	Feed inlet temperature [°C]	Circulation Flow rate [L/h]	Air gap manometric pressure [mbar]
1	60.0	400.0	-300.0
2	60.0	400.0	-500.0
3	60.0	600.0	-300.0
4	60.0	600.0	-500.0
5	70.0	400.0	-300.0
6	70.0	400.0	-500.0
7	70.0	600.0	-300.0
8	70.0	600.0	-500.0
9	56.6	500.0	-400.0
10	73.4	500.0	-400.0
11	65.0	331.8	-400.0
12	65.0	668.2	-400.0
13	65.0	500.0	-231.8
14	65.0	500.0	-568.2
15 (C)	65.0	500.0	-400.0
16 (C)	65.0	500.0	-400.0
17 (C)	65.0	500.0	-400.0

(C) – central point experiment.

In this experimental design matrix is showed the 8 runs of the 2^k factorial design (runs 1-8), 3 runs of central points and 6 axial runs (runs 9-14) to guarantee a stable variance within the experimental range.

This category of experimental design provides the analysis of curvature in the response surface when there is a maximum or minimum points in the experimental region. This type of experimental design is a low complexity method with few quantities of experiments that allows the evaluation of the experimental error at the expense of fewer runs than a complete design with replicates of type 3^k (Montgomery, 2012).

The evaluation of the production performance was performed by calculation of the distillate flux. This parameter was calculated as the ratio of the distillate volume rate by the membrane area available for evaporation, as presented in Eq. (1):

$$J_{Distillate}\left[\frac{L}{m^2 h}\right] = \frac{\dot{\phi}_{distillate}}{A_m}, \tag{1}$$

Where $J_{Distillate}$ is the distillate flux produced, $\dot{\phi}_{distillate}$ is the distillate volume rate and A_m is the effective membrane area.

As the membrane distillation process is thermally driven, the monitoring of energy efficiency-related performance parameters is also necessary. In this sense, the parameter *SECth* was verified (Eq. (2)), which quantifies the amount of energy required to produce 1 m^3 of distilled and GOR (Eq. (3)) defined as the ratio between the latent heat transported by water vapor through the membrane and the external heat added to the system:

$$SECth\left[\frac{kWh}{m^3}\right] = \frac{\dot{Q}_{ext}}{\dot{\phi}_{distilled}}, \tag{2}$$

Where *SECth* is the specific energy consumption, $\dot{Q}_{ext}$ is the external heat supplied and $\dot{\phi}_{distilled}$ is the is the distillate volumetric flow rate.

$$GOR = \frac{\dot{\phi}_{distilled}\ \rho_{distilled}\ \Delta h_{vap}}{\dot{Q}_{ext}}, \tag{3}$$

Where *GOR* is the gain output ratio, $\dot{Q}_{ext}$ is the external heat supplied, Δh_{vap} is the latent heat of vaporization, calculated based on (Ruiz-Aguirre et al. (2018), and $\rho_{distilled}$ is the density of distillate stream.

$$\dot{Q}_{ext}[kW] = CFR\rho_{\text{feed}}C_p\left(T_{in\_evap} - T_{out\_cool}\right), \tag{4}$$

Where $\dot{Q}_{ext}$ is the external heat supplied from the heat absorption circuit showed in Figure 1, *CFR* is the circulation flow rate of the saline solution in the pilot unit, C_p is the specific heat, T_{in_evap} is the inlet temperature into the feed channels, and T_{out_cool} is the outlet temperature from the cooling channels. The thermophysical properties of the feed stream were calculated according to the equations presented in El-Dessouky and Ettouney (2002) and considering the NaCl inlet concentration and the average value of T_{in_evap} and T_{out_cool}.

3. RESULTS AND DISCUSSION

The results presented below refer to membrane distillation experiments with a feed stream consisting of a NaCl solution with a nominal concentration of 35 g/L. The operational conditions were performed according to the experimental matrix of the central composite design (Table 1). The mean values of the response variables obtained for each set of at least three runs of each experimental condition performed are shown in Table 2. In all operating conditions studied, the cooling inlet temperature was selected to be 30 °C, and the deviation was less than ±1 °C. Because the operating mode of the pilot desalination unit in the V-AGMD configuration uses the feed salt solution itself as the cooling stream, the flow rate selected for the inlet of the cooling stream is the same as the inlet flow rate of the feed stream into the evaporation channels.

Considering 24 hours of operation and the values of the response variables of run 8, in which the highest average distillate flux was observed (1.8 L/m^2h), within the experimental ranges considered, a daily distillate production equivalent to 559.9 L was obtained with an external heat supply equal to 3.26 kWh. This demonstrated the production capacity of membrane distillation desalination in a pilot plant.

The software STATISTICA 14.0.0.15 (TIBCO©) was used for a better evaluation of the influence of the operational parameters (factors) on the performance parameters (response variables). This software provides a set of graphic tools for the analysis of Descriptive Statistics, Hypothesis Tests, distribution fitting, linear regression, and variance analysis for the experimental results. The values of the parameters: feed inlet temperature, circulation flow rate and air gap pressure

were considered as values of the experimental matrix Table 1 since input values should be equally spaced to respect the symmetry of the experimental design for the analysis in the software.

Based on the analysis of variance (ANOVA) of the results in Table 2 for the performance parameters, Pareto charts were obtained using t-test statistics for a significance level of $\alpha = 0.05$ for the average distillate flux ($J_{Destillate}$) (Figure 2a), specific thermal energy consumption (*SECth*) (Figure 2b) and gain output ratio (*GOR*) (Figure 2c).

Table 2. Experimental conditions and performance parameters in the experiments with NaCl solution (35 g/L) and cooling stream temperature selected to be 30 °C and with uncertainty expanded to a 95% confidence level.

Run	Feed inlet temperature $\pm U_{95\%}$ [°C]	Circulation flow rate $\pm U_{95\%}$ [L/h]	Air gap pressure $\pm U_{95\%}$ [mbar]	$J_{Distillate}$ $\pm U_{95\%}$ [L/m^{2}h]	*SECth* $\pm U_{95\%}$ [kWh/m^3]	*GOR* $\pm U_{95\%}$
1	60.0±0.3	400.0±2.7	-295.0±79.5	0.8±0.2	153.5±34.7	4.3±0.9
2	60.2±0.8	400.1±2.2	-499.8±22.0	0.8±0.1	142.9±10.0	4.6±0.3
3	60.0±0.3	600.1±3.2	-297.9±81.3	1.1±0.1	188.2±23.5	3.5±0.4
4	60.0±0.5	600.0±3.3	-496.7±44.3	1.2±0.1	169.4±14.0	3.9±0.3
5	70.0±0.2	400.0±3.8	-295.4±95.4	1.2±0.5	116.6±42.8	5.6±2.1
6	70.1±0.2	400.0±2.3	-498.7±24.5	1.2±0.1	114.9±7.6	5.7±0.4
7	70.1±0.2	599.9±4.0	-296.9±130.1	1.7±0.2	148.9±18.3	4.4±0.6
8	70.0±0.4	600.1±2.9	-495.6±47.0	1.8±0.1	140.0±7.2	4.7±0.2
9	56.6±0.3	500.0±2.7	-396.7±60.1	0.8±0.2	174.1±35.9	3.8±0.8
10	73.3±0.5	500.1±3.3	-397.9±36.7	1.6±0.1	134.7±6.9	4.8±0.3
11	65.0±0.2	332.0±2.5	-397.6±31.9	0.8±0.2	123.0±29.5	5.3±1.3
12	65.0±0.2	668.1±2.7	-393.7±78.9	1.6±0.4	171.4±42.3	3.8±1.0
13	65.1±0.1	500.0±3.2	-230.0±41.8	1.2±0.1	154.7±24.5	4.2±0.7
14	64.7±0.8	500.1±2.9	-566.4±28.5	1.2±0.1	143.3±5.8	4.6±0.2
15 (C)	65.0±0.2	500.0±3.0	-396.9±58.0	1.2±0.3	142.7±35.8	4.6±1.2
16 (C)	65.0±0.2	500.0±2.8	-399.6±18.5	1.2±0.1	148.9±5.3	4.4±0.2
17 (C)	65.1±0.4	500.0±2.8	-396.6±47.0	1.2±0.1	150.2±13.3	4.4±0.4

(C) – central point experiment.

The Pareto charts present the statistical significance of the evaluated factors and their interactions with respect to the response variables, which are the performance parameters, the values beside each rectangle refer to the values of the t-student statistic for each standardized effect estimate. The analysis of the Pareto charts allowed to infer that, in general, only the linear effects of the factors referring to feed inlet temperature and circulation flow rate were statistically significant for the experimental domain studied.

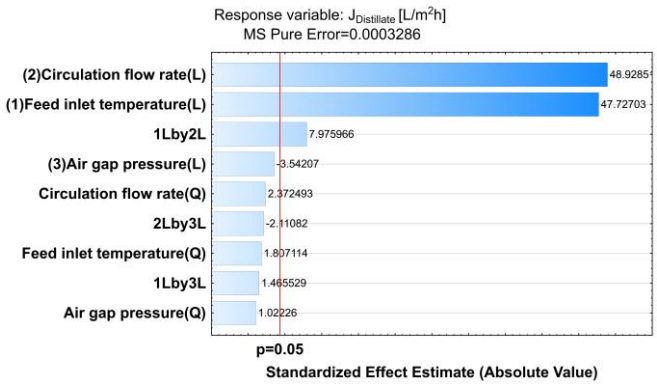

(a)

Figure 2. Pareto charts for the standardized effects central composite design for the performance parameters: (a) distillate flux, (b) specific thermal energy consumption (SECth), and (c) gain output ratio (GOR)

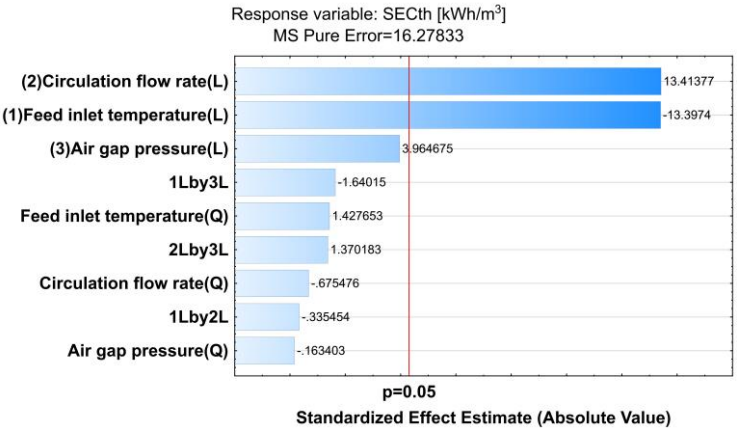

(b)

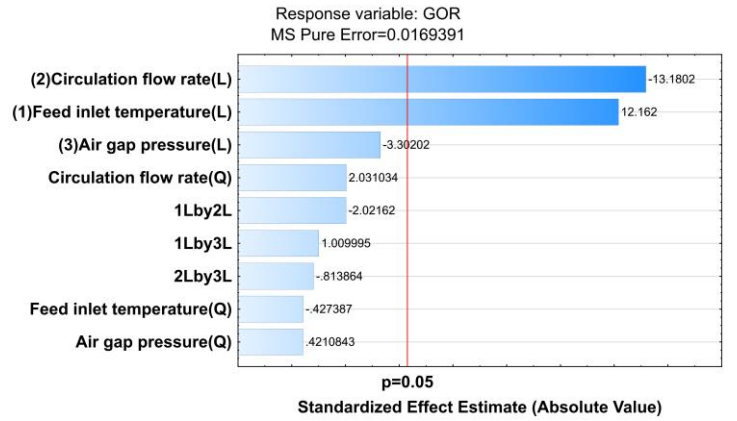

(c)

Figure 2. Pareto charts for the standardized effects central composite design for the performance parameters: (a) distillate flux, (b) specific thermal energy consumption (SECth), and (c) gain output ratio (GOR) (continued).

Table 3 shows the estimated normalized effects of the factors on the performance parameters studied. The highlighted values refer to the effects of the factors and their interactions that were statistically significant in the ANOVA.

As can be seen by analyzing the values presented in Table 3 and Figure 2a regarding the average distillate flux, increasing the circulation flow rate and the feed inlet temperature improves distillate production. Furthermore, the interaction of the linear effects of these two factors also appeared to be favorable for increasing the productivity of distilled water.

This behavior can be attributed to the influence that increased circulation flow has on the hydrodynamic, thermal, and mass boundary layer effects, reducing temperature and concentration polarization. In addition, the presence of spacers in the channels provides a greater influence of convective effects, and consequently, allowing higher temperatures at the interface of the membrane with the feed stream, favoring the evaporation process. Regarding the effect of the feed stream inlet temperature, this factor has a direct relationship with the driving force of the distillate flux, due to the relationship of the vapor pressure to the temperature of the feed stream at the interface with the membrane.

Ruiz-Aguirre et al. (2017) indicated that the increase in residence time, caused by the increase in the length of the channels in commercial modules, results in the reduction of the driving force across the membrane along the membrane length, one of the consequences being the observation of a linear increase in distillate flux as a function of the feed stream inlet temperature, in contrast to the exponential increase in distillate flux as a function of the feed stream inlet temperature observed in smaller laboratory-scale modules. Thus, for commercial spiral modules it is common to see lower distillate flux values than those obtained in laboratory modules for the same inlet temperatures of the feed stream.

Concerning the specific thermal energy consumption (*SECth*), the analysis of Figure 2b and Table 3 shows that the magnitudes of the effects of the factors related to circulation flow rate and feed inlet temperature are almost equal, although they have opposite effects. Increasing the feed inlet temperature decreases the *SECth* values. The effect of increasing this factor can be associated with higher distillate production due to the direct impact on the vapor pressure of the feed, thus decreasing the ratio between external heat supplied and the volume of distillate produced (Eq. (2)). Regarding the circulation flow rate factor, its increase causes *SECth* to grow due to an increment in the external heat supplied, as presented in Eqs. (2) and (4).

According to the study of Duong et al. (2016), increasing the circulation flow rate implies a reduction of the residence time in the module. Hence, there is a reduction in the time of the internal heat recovery step in the pilot module, which causes the system to present an increase in the consumption of external heat.

For the gain output ratio (*GOR*), it was verified by Figure 2c and Table 3 that the linear effects of the feed inlet temperature and the circulation flow had an opposite behavior to the one observed for *SECth*. For *GOR*, the circulation flow rate showed a negative linear effect, which can be justified by analyzing Eq. (3), in which the increase in external heat supplied, for the same water production, causes a reduction in *GOR* as the circulation flow rate is increased. Thus, the increase in GOR indicates that more external supplied heat energy is being effectively used in the evaporation of the water. For the feed inlet temperature, its increase causes a positive linear effect for the GOR values due to its contribution to the evaporation process.

Table 3. Normalized effects of the factors on the performance parameters studied.

Factor	Effects		
	Distillate flux [L/m²h]	**SECth [kWh/m³]**	**GOR**
Global mean	1.1975	147.5250	4.4496
(1) Feed inlet temperature (L)	0.4684	-29.2666	0.8570
Feed inlet temperature (Q)	0.0195	3.4369	-0.0332
(2) Circulation flow rate (L)	0.4800	29.2879	-0.9283
Circulation flow rate (Q)	0.0256	-1.6229	0.1574
(3) Air gap pressure (L)	-0.0347	8.6566	-0.2326
Air gap pressure (Q)	0.0110	-0.3926	0.0326
1L by 2L	0.1022	-0.9570	-0.1860
1L by 3L	0.0188	-4.6792	0.0929
2L by 3L	-0.0271	3.9090	-0.0749

Note: The highlighted values refer to the effects of the factors and their interactions that were statistically significant in the ANOVA; L – Linear effect; Q – Quadratic effect

Based on the model obtained by regression, resulting from the experimental design analysis and valid within the range of values selected for the factors studied, the response surface graphs shown in Figure 3 (*distillate flux*), Figure 4 (*SECth*), and Figure 5 (*GOR*) were obtained for the manometric pressures in the air gap of -300 mbar and -500 mbar.

The response surface plots for the mean distillate flux (Figure 3) confirm what was observed in the respective Pareto chart and the magnitude of the normalized effects, showing that the increase of the two statistically significant factors favors the distillate flux. The variation of the vacuum pressure inside the air gap in the distillate channels was not predominant in the analyzed response variable.

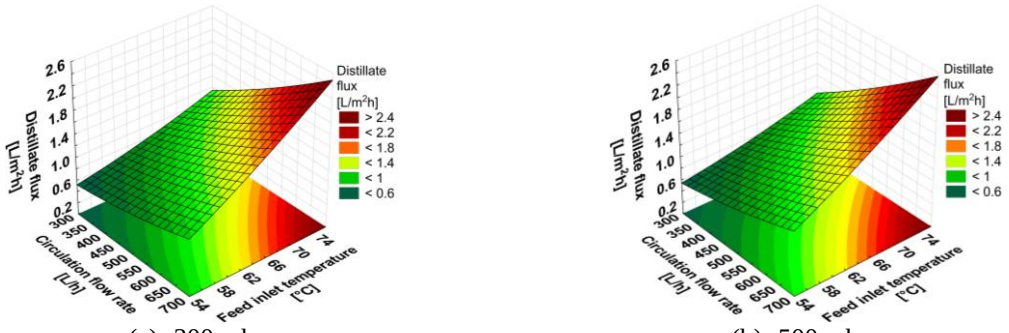

(a) -300 mbar (b) -500 mbar

Figure 3. Mean distillate flux as a function of feed inlet temperature and circulation flow rate for different air gap pressure.

In the analysis of the performance parameter regarding the specific thermal energy consumption (*SECth*), Figure 4 shows the decline in *SECth* caused by increasing the feed inlet temperature. Also, one can observe the increase in SECth with the rise in circulation flow rate.

For the gain output ratio (*GOR*), Figure 5 shows the response surface plots varying the feed inlet temperature and flow rate for different pressures in the air gap. In Figure 5, it is possible to observe that from the feed inlet temperature of 62 °C and for flow values lower than 550 L/h, the *GOR* value reaches the higher values within the studied operating conditions, which agrees with what was shown in the Pareto chart analysis about the significance of these factors.

Nevertheless, the intensification of the pressure reduction in the air gap did not significantly change the *GOR*, as was observed for the distillate flux and *SECth*.

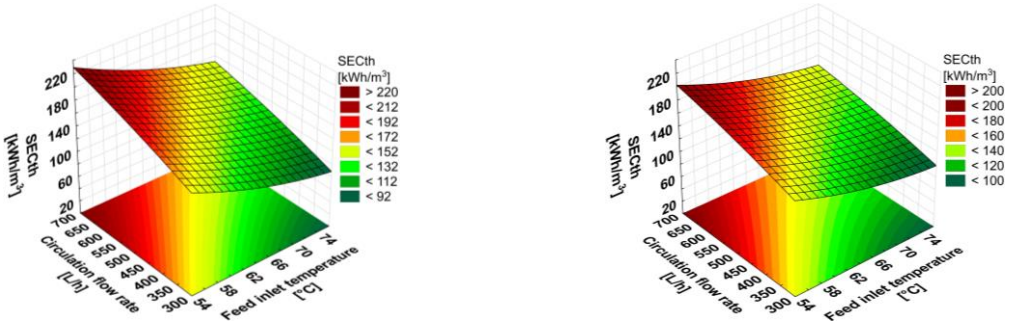

(a) -300 mbar (b) -500 mbar

Figure 4. Specific thermal energy consumption as a function of feed inlet temperature and circulation flow rate for different air gap pressure.

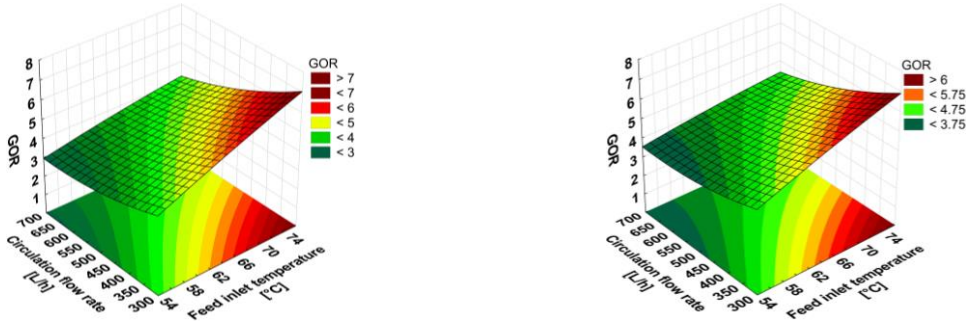

(a) -300 mbar (b) -500 mbar

Figure 5. Gain output ratio as a function of feed inlet temperature and circulation flow rate for different air gap pressure

3.1 Additional experiments with high concentration solutions

Complementary experiments were performed with a high concentration salt solutions (38.2±5 g/L and 66±5 g/L of NaCl) in order to preliminarily evaluate the ability of the membrane distillation module to process reject fluids from reverse osmosis (RO) desalination processes by offering an alternative to increase the water recovery rate and build the management of the desalination process rejects.

Figure 6 shows the distillate flux results obtained at the two concentration levels evaluated. Hence, it can be observed from Figure 6a and Figure 6b the effect of increasing the concentration that produces a reduction in the distillate flux. On the other hand, when the inlet temperature into the feed channel is increased from 65±2 °C to 74±2 °C and the circulation flow rate level from 300 L/h (Figure 6a) to 500 L/h (Figure 6b) there is an increase in the distillate flux, which agrees with the statistical analysis of variance (ANOVA) and the Pareto chart described previously by Figure 2a and Figure 3 in which these two factors are statistically significant and favor an increase in the distillate productivity.

It is worth emphasizing that the NaCl rejection coefficient for all experiments performed was greater than 91%, indicating a promising result in the quality of desalinated water obtained in the V-AGMD module, and the ability to process if residual solutions of high saline concentration as stated by Duong et al. (2015) and Bindels et al. (2020).

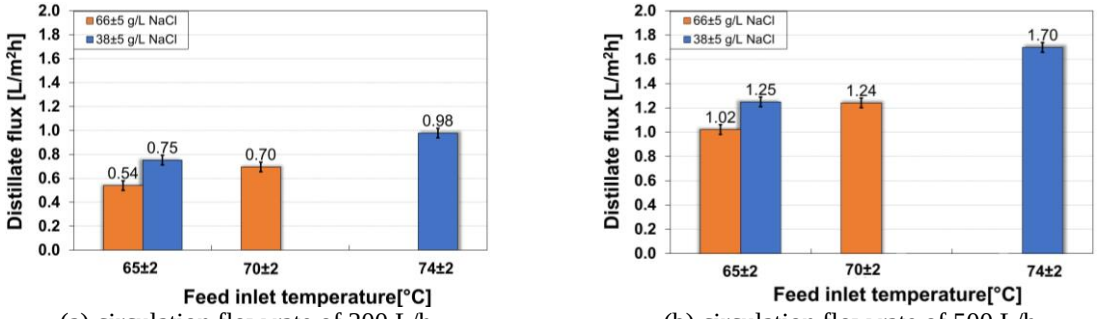

(a) circulation flow rate of 300 L/h (b) circulation flow rate of 500 L/h

Figure 6. Mean distillate flux as a function of feed inlet temperature for air gap pressure equal to -500 mbar

4. CONCLUSIONS

The presented study is part of the efforts to enhance the knowledge of the membrane distillation process at a pilot scale as an option to supply fresh water to isolated regions suffering from water scarcity. In this regard, a central composite experimental design was used to evaluate the effect of the operating parameters (factors): feed inlet temperature (56.6 °C - 73.4 °C), circulation flow rate (331.8 L/h - 668.2 L/h), and air gap manometric pressure (between -231.8 mbar and -568. 2 mbar) on the production performance (distillate flux) and thermal efficiency parameters (specific heat energy consumption and yield ratio) of the membrane distillation process of a 35 g/L NaCl solution (close to seawater) in a pilot system with a V-AGMD spiral module with membrane area equal to 12.96 m^2.

The statistical analysis of the performance parameters under the operating conditions guided by central composite design indicated that for the operational range of the analyzed factors, feed inlet temperature, circulation flow rate, and air gap pressure, only the first two factors presented statistical significance concerning the performance parameters considered as response variables: average distillate flux, specific thermal energy consumption and gain output ratio. For the distillate flux, the linear effects of the factors and their interactions concerning feed inlet temperature and circulation flow rate showed a positive influence on the increase of the distillate productivity.

For the specific thermal energy consumption, though, the increase of the feed inlet temperature showed a negative linear effect on the *SECth* values, and the circulation flow rate contributed positively to the enhancement of this parameter. Thus, to reduce the amount of external thermal energy required for distillate production, it was found to be advantageous to increase the feed inlet temperature.

Regarding the gain output ratio, this behavior is inverted. The effect of the circulation flow rate presented a negative contribution to the *GOR*, while the feed inlet temperature contributed to the increase of this parameter. For the parameters related to the thermal analysis of the process, the effect of the feed inlet temperature can be associated with its direct impact on the driving force of the process and the circulation flow rate is related to the amount of external heat supplied to produce distillate in the system. Furthermore, it was found that the vacuum intensity applied to the air gap in the distillate channel did not provide significant effects on the performance parameters considered within the selected operational range for the factors studied.

Conversely, additional experimental results with high concentration solutions showed NaCl rejection coefficients higher than 91%, indicating a promising result in the quality of desalinated water obtained in the V-AGMD module, and in verifying the ability to process residual solutions of high saline concentration such as those obtained in the rejects of desalination processes such as reverse osmosis (RO).

5. ACKNOWLEDGEMENTS

Partial funding by Petrogal-Brasil through ANP and EMBRAPII, PDI project no. GALP 38 with COPPETEC Foundation, and the sponsoring agencies CNPq, FAPERJ, and CAPES/PROCAD-Defesa, are gratefully acknowledged.

6. REFERENCES

Abu-Zeid, M. A. E. R., Zhang, L., Jin, W. Y., Feng, T., Wu, Y., Chen, H. L., and Hou, L., 2016. "Improving the performance of the air gap membrane distillation process by using a supplementary vacuum pump". *Desalination*, Vol. 384, p. 31–42.

Alsaadi, A. S., Francis, L., Maab, H., Amy, G. L., and Ghaffour, N., 2015. "Evaluation of air gap membrane distillation process running under sub-atmospheric conditions: Experimental and simulation studies". *Journal of Membrane Science*, Vol. 489, p. 73–80.

Andrés-Mañas, J. A., Requena, I., and Zaragoza, G., 2022. "Characterization of the use of vacuum enhancement in commercial pilot-scale air gap membrane distillation modules with different designs". *Desalination*, Vol. 528, p. 115490.

Andrés-Mañas, J. A., Ruiz-Aguirre, A., Acién, F. G., and Zaragoza, G., 2020. "Performance increase of membrane distillation pilot scale modules operating in vacuum-enhanced air-gap configuration". *Desalination*, Vol. 475, p. 114202.

Bahar, R., Ng, K. C., 2020. "Fresh water production by membrane distillation (MD) using marine engine's waste heat". *Sustainable Energy Technologies and Assessments*, Vol. 42, p. 100860.

Bindels, M., Carvalho, J., Gonzalez, C. B., Brand, N., and Nelemans, B., 2020. "Techno-economic assessment of seawater reverse osmosis (SWRO) brine treatment with air gap membrane distillation (AGMD)". *Desalination*, Vol. 489, p. 114532.

BRASIL, 2012, Programa Água Doce, Documento base (in Portuguese), Ministério do Meio Ambiente, Brasil. Available at: https://www.gov.br/mdr/pt-br/assuntos/seguranca-hidrica/programa-agua-doce/programa-agua-doce-1. Accessed 12 July 2023.

Chafidz, A., Al-Zahrani, S., Al-Otaibi, M. N., Hoong, C. F., Lai, T. F., and Prabu, M., 2014. "Portable and integrated solar-driven desalination system using membrane distillation for arid remote areas in Saudi Arabia". *Desalination*, Vol. 345, p. 36–49.

Deshmukh, A., Boo, C., Karanikola, V., Lin, S., Straub, A. P., Tong, T., Warsinger, D. M., and Elimelech, M., 2018. "Membrane distillation at the water-energy nexus: Limits, opportunities, and challenges". *Energy and Environmental Science*, Vol. 11, p. 1177–1196.

Duong, H. C., Cooper, P., Nelemans, B., Cath, T. Y., and Nghiem, L. D., 2016."Evaluating energy consumption of air gap membrane distillation for seawater desalination at pilot scale level". *Separation and Purification Technology*, Vol. 166, p. 55–62.

El-Dessouky and H. T., Ettouney, H. M., 2002. *Fundamentals of Salt Water Desalination*. Elsevier, Amsterdam.

Jones, E., Qadir, M., van Vliet, M. T. H., Smakhtin, V., and Kang, S. M., 2019. "The state of desalination and brine production: A global outlook". *Science of the Total Environment*. Vol. 657, p. 1343-1356.

Khayet, M. and Cojocaru, C., 2012. "Artificial neural network modeling and optimization of desalination by air gap membrane distillation". *Separation and Purification Technology*, Vol. 86, p. 171–182.

Khayet, Mohamed and Matsuura, T., 2011. *Membrane Distillation: Principles and Applications*. 1st. ed. Elsevier, Oxford.

Koschikowski, J., Wieghaus, M., and Rommel, M., 2003. "Solar thermal driven desalination plants based on membrane distillation". *Water Science and Technology: Water Supply*, Vol. 3, p. 49–55.

Montgomery, D. C., 2012. *Design and Analysis of Experiments*. 8th. ed. John Wiley & Sons, Inc.

Ong, C. L., Escher, W., Paredes, S., Khalil, A. S. G., and Michel, B., 2012. "A novel concept of energy reuse from high concentration photovoltaic thermal (HCPVT) system for desalination". *Desalination*, Vol. 295, p. 70–81.

Ruiz-Aguirre, A., Andrés-Mañas, J. A., Fernández-Sevilla, J. M., and Zaragoza, G., 2018. "Experimental characterization and optimization of multi-channel spiral wound air gap membrane distillation modules for seawater desalination". *Separation and Purification Technology*, Vol. 205, p. 212–222.

Ruiz-Aguirre, A., Andrés-Mañas, J. A., Fernández-Sevilla, J. M., and Zaragoza, G., 2017."Modeling and optimization of a commercial permeate gap spiral wound membrane distillation module for seawater desalination". *Desalination*, Vol. 419, p. 160–168.

Sanmartino, J. A., Khayet, M., García-Payo, M. C., El-Bakouri, H., and Riaza, A., 2017. "Treatment of reverse osmosis brine by direct contact membrane distillation: Chemical pretreatment approach", *Desalination*, Vol. 420, p. 79–90.

Sarbatly, R. and Chiam, C. K., 2013. "Evaluation of geothermal energy in desalination by vacuum membrane distillation". *Applied Energy*, Vol. 112, p. 737–746.

Schwantes, R., Chavan, K., Winter, D., Felsmann, C., and Pfafferott, J., 2018. "Techno-economic comparison of membrane distillation and MVC in a zero liquid discharge application". *Desalination*, Vol. 428, p. 50–68.

Wiesenfarth, M., Went, J., Bösch, A., Dilger, A., Kec, T., Kroll, A., Koschikowski, J., and Bett, A. W., 2016. "CPV-T mirror dish system combined with water desalination systems". In *12th International Conference on Concentrator Photovoltaic Systems - CPV-12*. Freiburg, Germany.

World Health Organization, 2017. *Guidelines for Drinking-water Quality: fourth edition incorporating the first addendum*. Geneva.

Yadav, A., Labhasetwar, P. K., Shahi, and V. K., 2021. "Membrane distillation using low-grade energy for desalination: A review", *Journal of Environmental Chemical Engineering*. Vol. 9, p. 105818.

7. RESPONSIBILITY NOTICE

The authors are the only responsible for the printed material included in this paper.